ELSEVIER

Available online at www.sciencedirect.com

SciVerse ScienceDirect

Ceramics International 39 (2013) 2975–2980

CERAMICS
INTERNATIONAL

www.elsevier.com/locate/ceramint

# Effect of CdSe quantum dots on the performance of hybrid solar cells based on ZnO nanorod arrays

Chongyu Zhu, Xinhua Pan, Chunli Ye, Lei Wang, Zhizhen Ye, Jingyun Huang*

*Department of Materials Science and Engineering, State Key Laboratory of Silicon Materials, Zhejiang University, Hangzhou 310027, PR China*

Received 16 August 2012; received in revised form 24 September 2012; accepted 24 September 2012
Available online 28 September 2012

## Abstract

This paper reports the fabrication and interface modification of hybrid inverted solar cells based on ZnO nanorod arrays and poly (3-hexylthiophene). CdSe quantum dots (QDs) are grafted to the ZnO nanorod array successfully by bifunctional molecule mercaptopropionic acid to enhance the device performance. The power conversion efficiency of the device is increased by 109% from 0.11% to 0.23% under simulated 1 sun AM 1.5 solar illumination at 100 mW/cm$^2$ after the modification. The grafting of CdSe QDs effectively enhanced the excition generation and dissociation on the organic/inorganic interface. This work may provide a general method for increasing the efficiency of organic–inorganic hybrid solar cells by interface modification.

*Keywords:* D. ZnO; Hybrid solar cell; Quantum dots; CdSe

## 1. Introduction

Organic/inorganic hybrid solar cells have attached a growing attention of researchers all over the world due to the advantage of light weight, potential low cost, flexibility from the organic materials, high mobility and stability from inorganic materials [1,2]. The application of inorganic 1-dimensional nano architectures, such as nanowire and nanoporous, have been researched in solar cells [3–6]. As the inorganic component of hybrid solar cells, wide band gap metal oxides, such as $TiO_2$, ZnO, $SnO_2$, and $Nb_2O_5$, have been tested for photovoltaic properties [7–9]. Among all the potential candidates, $TiO_2$ used to receive much attention and is still a widely used oxides in fabrication of variety patterns of solar cells [10–13]. Recently, ZnO received more attention due to its ideal characteristics such as low cost, non-toxicity and high stability as a novel inorganic material in hybrid solar cells. In particular, the electron mobility of ZnO is much higher than that of $TiO_2$, its main competitor [14–17]. In addition, ZnO nanorod arrays can be easily grown on different substrates by different methods, such as metal–organic chemical vapor deposition, magnetron sputtering, hydrothermal method, etc [18–21].

However, hydroxyl terminated metal oxides are known to act as electron charge traps, which can affect the electrical properties at the interface between the metal oxide and organic layers [22]. Improving the electrical coherence between these materials is important especially in polymer-based solar cells because the recombination losses at these interfaces can drastically affect the potential for photocurrent collection. Therefore, organic dyes and quantum dots (QDs) are widely used to modify the surface of ZnO crystals. QDs, such as CdS, CdSe, InP, InAs, $Bi_2S_3$, PbS, and $CuInS_2$, have advantages of tunable band gap in the visible region and better heterojunction formation with solid hole conductors over dye molecules [23–34]. Also, a unique potential capability of the QD-sensitized hybrid solar cell is generating multiple electron–hole pairs per photon by impact ionization (inverse Auger effect) [35]. These advantages make QDs effective sensitizers for wide band gap semiconductor materials used in solar cells in lieu of photosensitive dyes.

---

*Corresponding author. Tel.: +86 571 87952118; fax: +86 571 87952625.
*E-mail address:* huangjy@zju.edu.cn (J. Huang).

0272-8842/\$ - see front matter © 2012 Elsevier Ltd and Techna Group S.r.l. All rights reserved.
http://dx.doi.org/10.1016/j.ceramint.2012.09.074

Herein, we reported the fabrication of vertical hybrid solar cells with ZnO nanorod arrays-CdSe QDs core-shell architectures and P3HT. The p-n heterojunctions between the n-type CdSe QDs and the p-type P3HT effectively realize the efficient charge separation process. In addition, the energy band structure of the interface between CdSe QDs and ZnO can also promote the separation of electron–hole pairs. ZnO nanorod arrays, which provide direct channels for electron transport to the electrodes, play the role of the electron collection material. Due to the property of intrinsic n-type of ZnO, ZnO nanorod arrays are also used as the hole blocking layer of the hybrid solar cells.

## 2. Experimental

### 2.1. Synthesis of ZnO nanorods and CdSe QDs

ZnO nanorod arrays were prepared by magnetron sputtering and hydrothermal method. A 80 nm thick layer of ZnO was sputtered to the ITO substrates as the seed layer by magnetron sputtering in argon atmosphere under the pressure of 0.65 Pa, with the reflected power of 100 W. To grow ZnO nanorod arrays on the prepared seed layer, 0.35 g hexamethylenetetramine, 0.74 g $Zn(NO_3)_2$ and 100 ml deionized water were added into the hydrothermal reactor and the mixture was heated to 95 °C for 90 min.

CdSe QDs were synthesized by the hot-injection method described in the literature [36]. In a typical synthetic process, 76 mg CdO, 3.0 g trioctylphosphine oxide (TOPO) and 3.0 ml oleic acid were added into the reactor and the mixture was heated to higher than 280 °C under vigorous stirring in the nitrogen atmosphere. 80 mg of Se was added into 1.0 ml of trioctylphosphine (TOP) and ultrasonicated until the solution became clear. Then the Se-TOP solution was quickly injected into the mixture of CdO, TOPO and oleic acid. After 5 min reaction, the hot solution was quickly transferred into 5 ml toluene. The as-prepared CdSe QDs were washed in methanol and separated by centrifugation for two times. The CdSe QDs were then dispersed in 15 ml pyridine and stirred for 24 h in nitrogen. The resulting nanocrystals were washed by hexane and separated by centrifugation. The final products were dried by blow of nitrogen.

### 2.2. Device fabrication

The freshly prepared ZnO coated indium thin oxide (ITO) substrates were heated at 150 °C for 20 min and cooled down with nitrogen flow. For CdSe QDs grafted ones, ZnO nanorod arrays were immersed in 0.1 M mercaptopropionic acid (MPA) in ethanol for 10 h, and rinsed by pure ethanol. Then the samples were immersed in 5 mg/ml CdSe QDs solution in toluene for 15 min and rinsed by pure toluene. 36 mg/ml P3HT (Luminescence Technology Corp.) solutions in dichlorobenzene (Aldrich) was spin-coated at 500 rpm for 60 s. After deposition, the samples were annealed at 225 °C in glove box for 60 s to enhance infiltration into the nanorods and to enhance the crystallinity of the P3HT. Subsequently, samples were loaded into a vacuum deposition chamber (background pressure $\approx 5 \times 10^{-4}$ Pa) to deposit 10 nm $MoO_3$ and 100 nm aluminum as cathode with a shadow mask (device area of 9 $mm^2$).

### 2.3. Device characterization

The current density–voltage (J–V) curves were measured with Keithley 236 measurement source units at room temperature in air. The photocurrent was measured under a calibrated solar simulator (Abet 300 W) at 100 $mW/cm^2$, and the light intensity was calibrated with a standard photovoltaic (PV) reference cell. External quantum efficiency (EQE) spectrum was measured with Stanford lock-in amplifier 8300 unit.

The morphologies of ZnO nanorods and CdS nanorods/P3HT hybrid films were observed on a Hitachi S-4800 field-emission scanning electron microscope (FESEM). UV–vis absorption spectra were obtained using a UV-2450 UV–vis Shimadzu spectrophotometer. The steady-state photoluminescence (PL) spectra were taken on a FluoroMax-4 HORIBA Jobin Yvon spectrofluorometer. The morphological structures of CdSe QDs were investigated on a carbon-coated copper grid by the CM200 transmission electron microscope (TEM) at 160 KV.

## 3. Results and discussion

ZnO nanorod arrays were fabricated on patterned ITO-coated glass substrates with a sheet resistance of 10 Ω/sqr. The CdSe QDs was synthesized according to the literature. Fig. 1a and b show the SEM top view of ZnO nanorod arrays and cross-section SEM images of P3HT/CdSe QDs/ZnO nanorods structure, respectively. The ZnO nanorods are 80 nm in diameter and about 400 nm long. It is apparent that we realized ideal infiltration of P3HT into the arrays by spin-coating and annealing, which is very important to realize high-efficiency hybrid solar cells. Fig. 2a shows the TEM images of the synthesized CdSe QDs, we can find their spherical shape and well controlled size distribution. In our work, a bifunctional molecule, MPA, was used to graft CdSe QDs to the ZnO nanorods, because of the high affinity of –COOH to the ZnO and –SH to CdSe. The optical absorption properties of the CdSe QDs were preserved when the QDs were attached to the ZnO nanorod. Fig. 2b shows the absorption spectrum of ZnO nanorod, CdSe QDs, CdSe QDs grafted ZnO nanorod and P3HT films. The onset of the absorption spectrum of CdSe QDs treated ZnO nanorod by MPA was 660 nm as that of CdSe QDs, which strongly indicates that CdSe QDs was successfully grafted to the ZnO nanorod.

The device architecture of the investigated P3HT/CdSe QDs/ZnO nanorods hybrid solar cells and its relevant band diagram are shown in Fig. 3a and b. The energy band structure of the device provides an ideal environment for carriers' directional transfer to the electrode. Fig. 4a shows a dramatically improved photovoltaic response of devices after grafting CdSe QDs to the ZnO nanorods. The photovoltaic performance parameters short-circuit current density (Jsc), open-circuit potential (Voc), fill factor (FF) and power conversion efficiency (PCE) of these corresponding devices are summarized in Table 1. Compared to the device without grafting CdSe QDs, the surface modification leads to a 118% increase of Jsc from $0.66 \pm 0.06$ mA/cm$^{-2}$ to $1.44 \pm 0.25$ mA/cm$^{-2}$, a 12.5% increase of Voc from 0.32 V to 0.36 V. However, the FF decreases from $0.53 \pm 0.02$ to $0.43 \pm 0.03$, which may due to the long-chain surfactants in the surface of CdSe QDs. The increase of series resistance (Rs) from 23.1 $\Omega$ cm$^2$ to 50.8 $\Omega$ cm$^2$ when the ZnO nanorods were modified by long-chain surfactants capped CdSe QDs indicate that the ligands may act as charge traps or prevent charge transport [37,38]. These ligands always act as charge traps or prevent charge transport. Overall, these changes improve the PCE from $0.11 \pm 0.01\%$ to $0.23 \pm 0.03\%$, with an overall improvement of 109%. The external quantum efficiencies (EQE) with or without grafted CdSe QDs are compared in Fig. 4b. The device for CdSe QDs grafted ZnO nanorods shows much higher EQE values covering the whole absorption range with a maximum value of approximately 15% at around 500 nm, which is consistent with its much higher Jsc.

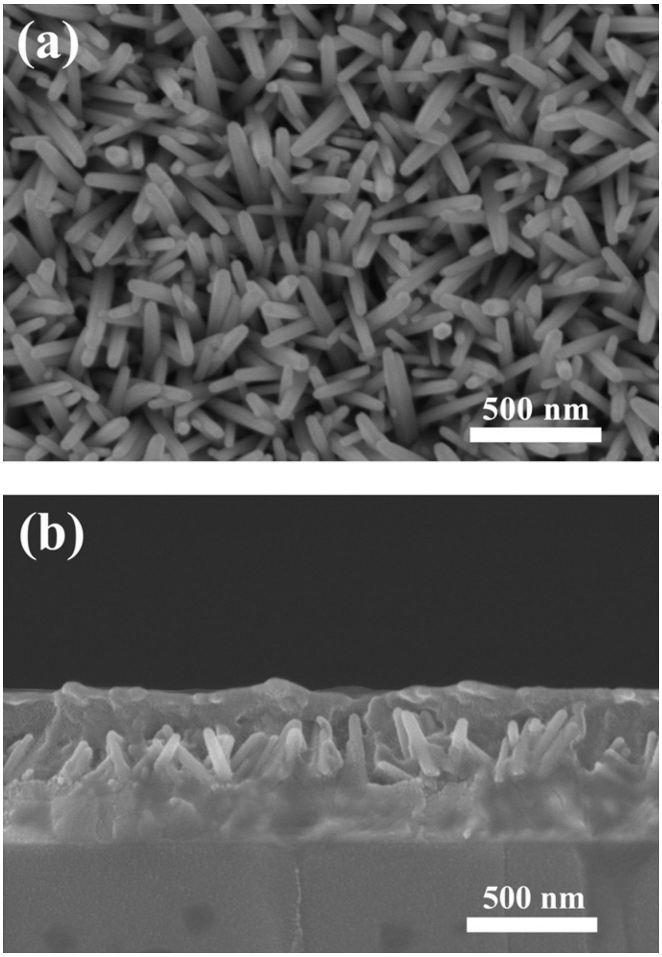

Fig. 1. a) Top view of ZnO nanorod arrays; b) cross-section SEM images of CdSe QDs grafted ZnO nanorod arrays coated by P3HT, annealed at 225 °C for 60 s.

The device performance enhancement may result from the improvement of the CdSe/P3HT interface. To have a deeper understanding of the origin of the performance improvement of the hybrid solar cells after grafting CdSe QDs, we investigated the exciton generation and dissociation process of the hybrid films. Fig. 5a shows the absorption spectra of ZnO/P3HT hybrid and ZnO/CdSe QDs/P3HT hybrid films. It is observed that the absorption of the hybrid films in the all range of 300–650 nm is enhanced after grafting CdSe QDs, which means CdSe QDs contributed to the optical absorption and excition generation process. Hence, the improved photovoltaic performance should be partially caused by the absorption enhancement of the hybrid films. This enhancement may be due to the unique multiple electron–hole pairs generating progress of QDs and the relatively larger specific interface area between CdSe QDs and P3HT. Fig. 5b shows photoluminescence (PL) emission spectra of ZnO/

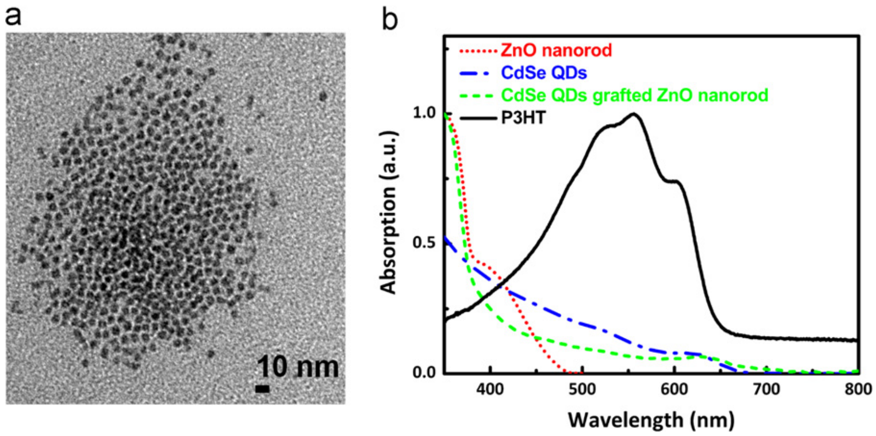

Fig. 2. a) TEM images of the synthesized CdSe QDs; b) UV–vis absorption of ZnO nanorod, CdSe QDs, CdSe QDs grafted ZnO nanorod and P3HT films.

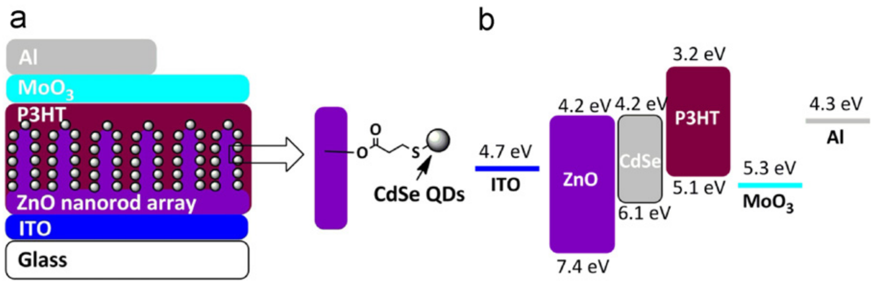

Fig. 3. a) Schematic of the ITO/ZnO naonorods/CdSe QDs/MoO3/Al hybrid solar cells and b) energy level diagram of the corresponding device.

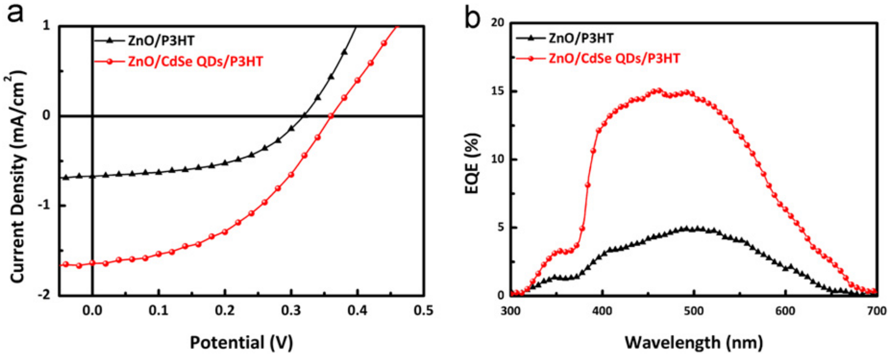

Fig. 4. a) Current density–voltage (J–V) characteristics under simulated 1 sun AM 1.5 solar illumination and b) External quantum efficiency (EQE) for hybrid solar cells for ZnO nanorods with or without CdSe QDs.

Table 1
Summary of photovoltaic performance of solar cells. The average parameters are based on the six devices on the same substrate.

| Active layer | Voc/V | Jsc/(mA/cm$^2$) | FF | PCE (%) | Rs[a] (Ω cm$^2$) |
|---|---|---|---|---|---|
| ZnO/P3HT | 0.32 | $0.66 \pm 0.06$ | $0.53 \pm 0.02$ | $0.11 \pm 0.01$ | 23.1 |
| ZnO/CdSe QDs/P3HT | 0.36 | $1.44 \pm 0.25$ | $0.43 \pm 0.03$ | $0.23 \pm 0.03$ | 50.8 |

[a] Series resistance (Rs) for solar cells under illumination is obtained at 1 V in the J–V curves.

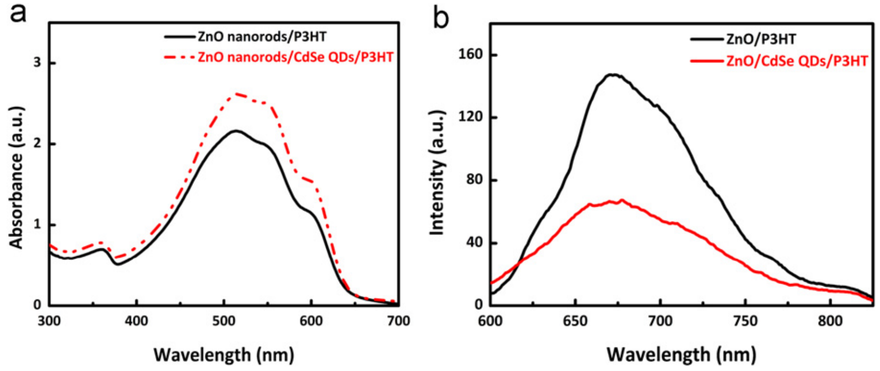

Fig. 5. a) UV–vis absorption spectra of ZnO/P3HT hybrid and ZnO/CdSe QDs/P3HT hybrid; b) PL emission spectra of ZnO/P3HT hybrid and CdS/CdSe QDs/P3HT hybrid.

P3HT hybrid and ZnO/CdSe QDs/P3HT hybrid films. The PL intensity is significantly reduced after grafting CdSe QDs. It shows a weaker exciton recombination process. Taking into account the increased optical absorption, we can tell that more efficient exciton dissociation was achieved at the organic/inorganic interface.

## 4. Conclusion

In summary, hybrid inverted solar cells based on ZnO nanorod arrays and P3HT were fabricated. We have found that bifunctional molecule MPA can effectively graft CdSe QDs to the ZnO nanorods. This modification of the interface between the inorganic ZnO and the organic P3HT layer can improve the performance of solar cells by 109% due to the exciton generation and dissociation enhancement. This work may provide a useful method to achieve high performance organic–inorganic hybrid solar cells by interface modification.

## Acknowledgment

This work was partly supported by the National Natural Science Foundation of China, Innovation key team of Zhejiang province under grant no.2010R50020 and the Doctorate Fund of the Ministry of Education under grant no. 2011010110013.

## References

[1] W.U. Huynh, J.J. Dittmer, A.P. Alivisatos, Hybrid nanorod–polymer solar cells, Science 295 (2002) 2425–2427.

[2] M. Helgesen, R. Sondergaard, F.C. Krebs, Advanced materials and processes for polymer solar cell devices, Journal of Materials Chemistry 20 (2010) 36–60.

[3] E.C. Garnett, P.D. Yang, Silicon nanowire radial p-n junction solar cells, Journal of the American Chemical Society 130 (2008) 9224–9225.

[4] M. Law, L.E. Greene, J.C. Johnson, R. Saykally, P.D. Yang, Nanowire dye-sensitized solar cells, Nature Materials 4 (2005) 455–459.

[5] M. Zhong, D. Yang, J. Zhang, J.Y. Shi, X.L. Wang, C. Li, Improving the performance of CdS/P3HT hybrid inverted solar cells by interfacial modification, Solar Energy Materials and Solar Cells 96 (2012) 160–165.

[6] Y. Myung, J.H. Kang, J.W. Choi, D.M. Jang, J. Park, Polytypic ZnCdSe shell layer on a ZnO nanowire array for enhanced solar cell efficiency, Journal of Materials Chemistry 22 (2012) 2157–2165.

[7] K. Sayama, H. Sugihara, H. Arakawa, Photoelectrochemical properties of a porous $Nb_2O_5$ electrode sensitized by a ruthenium dye, Chemistry of Materials 10 (1998) 3825–3832.

[8] S. Ferrere, A. Zaban, B.A. Gregg, Dye sensitization of nanocrystalline tin oxide by perylene derivatives, Journal of physical chemistry B 101 (1997) 4490–4493.

[9] K. Keis, J. Lindgren, S.E. Lindquist, A. Hagfeldt, Studies of the adsorption process of Ru complexes in nanoporous ZnO electrodes, Langmuir 16 (2000) 4688–4694.

[10] H.G. Bang, J.K. Chung, R.Y. Jung, S.Y. Park, Effect of acetic acid in $TiO_2$ paste on the performance of dye-sensitized solar cells, Ceramics International 38 S (2012) S511–S515.

[11] Y.S. Jin, K.H. Kim, W.J. Kim, K.U. Jang, H.W. Choi, The effect of RF-sputtered $TiO_2$ passivating layer on the performance of dye sensitized solar cells, Ceramics International 38 S (2012) S505–S509.

[12] A.T. Raghavender, A.P. Samantilleke, Pedro Sa, B.G. Almeida, M.I. Vasilevskiy, Nguyen Hoa Hong, Simple way to make anatase $TiO_2$ films on FTO glass for promising solar cells, Materials Letters 69 (2012) 59–62.

[13] E.C. Muniz, M.S. Góes, J.J. Silva, J.A. Varela, E. Joanni, R. Parra, P.R. Bueno, Synthesis and characterization of mesoporous $TiO_2$ nanostructured films prepared by a modified sol–gel method for application in dye solar cells, Ceramics International 37 (2011) 1017–1024.

[14] M. Quintana, T. Edvinsson, A. Hagfeldt, G. Boschloo, Comparison of dye-sensitized ZnO and $TiO_2$ solar cells: studies of charge transport and carrier lifetime, Journal of Physical Chemistry C 111 (2007) 1035–1041.

[15] T.W. Hamann, A.B.F. Martinson, J.W. Elam, M.J. Pellin, J.T. Hupp, Aerogel templated ZnO dye-sensitized solar cells, Advanced Materials 20 (2008) 1560–1564.

[16] D. Niinobe, Y. Makari, T. Kitamura, Y. Wada, S. Yanagida, Origin of enhancement in open-circuit voltage by adding ZnO to nanocrystalline $SnO_2$ in dye-sensitized solar cells, Journal of Physical Chemistry B 109 (2005) 17892–17900.

[17] J.B. Cui, Defect control and its influence on the exciton emission of electrodeposited ZnO nanorods, Journal of Physical Chemistry C 112 (2008) 10385–10388.

[18] A.M. Lockett, P.J. Thomas, P. O'Brien, Influence of seeding layers on the morphology, density, and critical dimensions of ZnO nanostructures grown by chemical bath deposition, Journal of Physical Chemistry C 116 (2012) 8089–8094.

[19] J.P. Liu, X.T. Huang, Y.Y. Li, X.X. Ji, Z.K. Li, X. He, F.L. Sun, Vertically aligned 1D ZnO nanostructures on bulk alloy substrates: direct solution synthesis, photoluminescence, and field emission, Journal of Physical Chemistry C 111 (2007) 4990–4997.

[20] L. Vayssieres, Growth of arrayed nanorods and nanowires of ZnO from aqueous solutions, Advanced Materials 15 (2003) 464–466.

[21] L.Y. Chen, Y.T. Yin, C.H. Chen, J.W. Chiou, Influence of polyethyleneimine and ammonium on the growth of ZnO nanowires by hydrothermal method, Journal of Physical Chemistry C 115 (2011) 20913–20919.

[22] S.K. Hau, Y.J. Cheng, H.L. Yip, Y. Zhang, H. Ma, A.K.Y. Jen, Effect of chemical modification of fullerene-based self-assembled monolayers on the performance of inverted polymer solar Cells, Applied Materials and Interfaces 2 (2010) 1892–1902.

[23] P.V. Kamat, Quantum dot solar cells. Semiconductor nanocrystals as light harvesters, Journal of Physical Chemistry C 112 (2008) 18737–18753.

[24] R. Vogel, K. Pohl, H. Weller, Sensitization of highly porous, polycrystalline $TiO_2$ electrodes by quantum sized CdS, Chemical Physics Letters 174 (1990) 241–246.

[25] R. Vogel, P. Hoyer, H. Weller, Quantum-sized PbS, CdS, $Ag_2S$, $Sb_2S_3$, and $Bi_2S_3$ particles as sensitizers for various nanoporous wide-bandgap semiconductors, Journal of Physical Chemistry 98 (1994) 3183–3188.

[26] R. Saurez, P.K. Nair, P.V. Kamat, Photoelectrochemical behavior of $Bi_2S_3$ nanoclusters and nanostructured thin films, Langmuir 14 (1998) 3236–3241.

[27] L.M. Peter, K.G.U. Wijayantha, D.J. Riley, J.P. Waggett, Band-edge tuning in self-assembled layers of $Bi_2S_3$ nanoparticles used to photosensitize nanocrystalline $TiO_2$, Journal of Physical Chemistry B 107 (2003) 8378–8381.

[28] B. Farrow, P.V. Kamat, CdSe quantum dot sensitized solar cells. Shuttling electrons through stacked carbon nanocups, Journal of the American Chemical Society 131 (2009) 11124–11131.

[29] D. Liu, P.V. Kamat, Photoelectrochemical behavior of thin cadmium selenide and coupled titania/cadmium selenide semiconductor films, Journal of Physical Chemistry 97 (1993) 10769–10773.

[30] I. Robel, V. Subramanian, M. Kuno, P.V. Kamat, Quantum dot solar cells. Harvesting light energy with CdSe nanocrystals molecularly linked to mesoscopic $TiO_2$ films, Journal of the American Chemical Society 128 (2006) 2385–2393.

[31] H.J. Lee, J.H. Yum, H.C. Leventis, S.M. Zakeeruddin, S.A. Haque, P. Chen, S.I. Seok, M. Grätzel, M.K. Nazeeruddin, CdSe quantum dot-sensitized solar cells exceeding efficiency 1% at full-sun intensity, Journal of Physical Chemistry C 112 (2008) 11600–11608.

[32] A. Zaban, O. Mićić, B.A. Gregg, A.J., Photosensitization of nanoporous $TiO_2$ electrodes with InP quantum dots, Nozik, Langmuir. 14 (1998) 3153–3156.

[33] O. Niitsoo, S.K. Sarkar, C. Pejoux, S. Rühle, D. Cahen, G. Hodes, Chemical bath deposited CdS/CdSe-sensitized porous $TiO_2$ solar cells, Journal of Photochemistry and Photobiology 181 (2006) 306–313.

[34] P. Yu, K. Zhu, A.G. Norman, S. Ferrere, A.J. Frank, A.J. Nozik, Nanocrystalline $TiO_2$ solar cells sensitized with InAs quantum dots, Journal of Physical Chemistry B 110 (2006) 25451–25454.

[35] A.J. Nozik, Quantum dot solar cells, Physica E 14 (2002) 115–120.

[36] L. Qian, J.H. Yang, R.J. Zhou, A.W. Tang, Y. Zheng, T.K. Tseng, D. Bera, J.G. Xue, P.H. Holloway, Hybrid polymer-CdSe solar cells with a ZnO nanoparticle buffer layer for improved efficiency and lifetime, Journal of Materials Chemistry 21 (2011) 3814–3817.

[37] J. Yang, A. Tang, R. Zhou, J. Xue, Effects of nanocrystal size and device aging on performance of hybrid poly(3-hexylthiophene): CdSe nanocrystal solarcells, Solar Energy Materials and Solar Cells 95 (2011) 476–482.

[38] Y. Wu, G. Zhang, Performance enhancement of hybrid solar cells through chemical vapor annealing, Nano Letters 10 (2010) 1628–16.